SHORT THESIS FOR THE DEGREE OF DOCTOR OF PHILOSOPHY (PHD)

Investigation of the effects of factor XIII on the cellular functions of vascular smooth muscle cells and of α2-plasmin inhibitor heterogeneity on fibrinolysis

by Réka Kissné Bogáti

Supervisor: Éva Katona, PhD

UNIVERSITY OF DEBRECEN
KÁLMÁN LAKI DOCTORAL SCHOOL

DEBRECEN, 2026

Investigation of the effects of factor XIII on the cellular functions of vascular smooth muscle cells and of α2-plasmin inhibitor heterogeneity on fibrinolysis

By **Réka Kissné Bogáti** (MSc degree)

Supervisor: **Éva Katona, PhD**

Kálmán Laki Doctoral School, University of Debrecen

Head of the **Examination Committee**:	Prof. György Balla, MD, PhD, DSc, MHAS
Members of the Examination Committee:	Ágnes Simon, MD, PhD
	Róbert Király, PhD

The Examination takes place at the Library of the Division of Clinical Laboratory Science, Department of Laboratory Medicine, Faculty of Medicine, University of Debrecen, at 12:30 pm, 11th of May, 2026.

Head of the **Defense Committee**:	Prof. György Balla, MD, PhD, DSc, MHAS
Reviewers:	Dániel Törőcsik, MD, PhD, DSc
	Anna Tanka-Salamon, PhD

Members of the Defense Committee:	Prof. György Balla, MD, PhD, DSc, MHAS
	Ágnes Simon, MD, PhD
	Dániel Törőcsik, MD, PhD, DSc
	Róbert Király, PhD
	Anna Tanka-Salamon, PhD

The PhD Defense takes place at the Lecture Hall of Bldg. A, Department of Internal Medicine, Faculty of Medicine, University of Debrecen, at 2:00 pm, 11th of May, 2026.

1. INTRODUCTION

Hemostasis is responsible for maintaining the liquid state of blood circulating within the vascular system and for the formation of blood clots in the event of vascular wall damage. Under normal conditions, this complex regulatory system is capable of simultaneously controlling coagulation and fibrinolysis in cooperation with numerous components. Key components of the system are blood cells (platelets, red blood cells, and white blood cells), special proteins with different functions (coagulation and fibrinolytic), and tissue factors that make up the vessel wall (cell surface receptors, membrane proteins, and various types of tissue cells). Active factor XIII (FXIIIa) plays a significant role in hemostasis, wound healing, angiogenesis, and presumably also in the process of atherosclerosis. By forming cross-links between various integrins and growth receptors on the cell surface, it is able to activate signaling pathways, enhancing the migration, proliferation, and survival of endothelial cells, fibroblasts, and monocytes. Furthermore, through cross-links formed in the extracellular matrix, it also influences the maintenance of matrix stability. In addition to playing an important role in hemostasis by forming stable fibrin clots through cross-linking fibrin chains, FXIIIa also participates in the regulation of fibrinolysis by binding the main inhibitor of plasmin, α2-plasmin inhibitor (α2PI), the main inhibitor of plasmin, to the fibrin α-chain via a covalent bond, protecting it from early degradation by plasmin. α2PI forms an irreversible complex (PAP complex) with free circulating plasmin in plasma. α2PI circulates in plasma in several isoforms as a result of proteolytic cleavages affecting both ends of the molecule. These modifications may influence the role of α2PI in fibrinolysis. The function of the N-terminally truncated form has been studied by several research groups, but little is currently known about C-terminal modifications. The C-terminally cleaved form (NPB-α2PI) loses its plasminogen binding site and is therefore much slower to inhibit plasmin, and FXIIIa is primarily able to cross-link fibrin with the plasminogen-binding, uncleaved form (PB-α2PI). The effect of the NPB-α2PI form on fibrinolysis has been less studied.

In this paper, we summarize our findings on the effects of factor XIII (FXIII) on the functions of human aortic smooth muscle cells (HAoSMCs). Furthermore, we investigated the effect of α2PI heterogeneity on the extent of α2PI incorporation into fibrin clots, as well as on clot structure and lysis.

2. REVIEW OF LITERATURE

2.1 Structure and activation of coagulation factor XIII

Coagulation factor XIII (FXIII) is a protransglutaminase, of which two forms are known: the plasma form (pFXIII) and the cellular form (cFXIII). In plasma, it exists as a heterotetramer composed of two potentially active A subunits (FXIII-A) and two carrier/inhibitory B subunits (FXIII-B), with a plasma concentration of 14–28 mg/L.

FXIII-A has a molecular weight of 83 kDa and consists of 732 amino acids. It is composed of four structural domains: β-sandwich, catalytic core, β-barrel 1, and β-barrel 2. At its N-terminal end, a 37-amino-acid activation peptide (AP-FXIII) is involved in FXIII activation, as well as in Ca^{2+} binding. The cellular form of FXIII is a homodimer composed of two A subunits (FXIII-A_2). It has been detected in several cell types, including platelets, monocytes/macrophages, osteoblasts, osteoclasts, osteocytes, chondrocytes, and corneal keratocytes. The A subunit that enters the plasma mainly originates from resident tissue macrophages, 99% of it forms a complex with the B subunit and circulates bound to fibrinogen.

FXIII-B is a glycoprotein of ~80 kDa, consisting of 641 amino acids, synthesized by hepatocytes. About 50% circulates in complex with FXIII-A, while the other 50% is present in free form in plasma. Each of its ten short tandem repeat “sushi” domains is stabilized by two disulfide bonds. Its main function is to prolong the half-life of FXIII-A_2 in circulation, protecting it from spontaneous activation and degradation. In plasma, both the FXIII-A_2B_2 complex and free FXIII-B circulate bound to fibrinogen. Binding to fibrinogen plays a major role in FXIII activation. Casini and colleagues reported that in afibrinogenemia, despite normal levels of FXIII-A_2B_2, only about 18% activity can be detected.

The zymogen heterotetramer FXIII (FXIII-A_2B_2), with a molecular weight of 326 kDa, is converted into active transglutaminase (FXIIIa) in the presence of thrombin and Ca^{2+} during the final phase of coagulation. In the first step of the process, thrombin cleaves the activation peptide located at the N-terminal region of the FXIII-A subunit through peptide bond hydrolysis, thereby weakening the connection between the two FXIII subunits. Subsequently, in the presence of Ca^{2+}, the B subunits dissociate, resulting in the enzymatically active form of the FXIII-A subunits. Activation occurs on the surface of polymerizing fibrin, which accelerates thrombin-mediated AP-FXIII cleavage approximately 100-fold and facilitates dissociation of the FXIII-B subunits.

Proteolytic cleavage is not required for cellular FXIII activation; an intracellularly elevated Ca^{2+} concentration above 2 mM is sufficient. A 2014 study has described that cFXIII retains its activity when it moves from the cytoplasm of platelets to the cell surface. FXIII-A2, circulating in its free form in the plasma, can also be activated by cleavage of the activation peptide in the presence of Ca^{2+}.

2.2 Functions of FXIII

2.2.1 The role of FXIII in blood coaguation

FXIIIa catalyzes an acyl-transfer reaction, during which a strong, stable, proteolysis-resistant isopeptide bond is formed between the γ-carboxamide group of a glutamine side chain in one (donor) protein and the ε-amino group of a lysine side chain in another (acceptor) protein. FXIIIa cross-links the α- and γ-chains of fibrin, thereby promoting fibrin γ–γ dimers, γ–α, and α–α polymers, which contribute to the formation of a stable fibrin clot, playing a crucial role in hemostasis. In addition, FXIIIa covalently binds the main inhibitor of plasmin, α2-plasmin inhibitor (α2PI), to the fibrin α-chain, preventing premature degradation of the fibrin network by plasmin. Patients with FXIII-A deficiency suffer from severe bleeding symptoms.

2.2.2 The role of FXIII in angiogenesis, wound healing, and atherosclerosis

During angiogenesis, new capillaries form, promoting tissue formation and wound healing. The blood vessel walls and capillaries consist of three layers (intima, media, adventitia), composed of cells of different types and functions: endothelial cells, vascular smooth muscle cells (VSMC), and fibroblasts.

VSMCs can migrate from the medial layer of the vessel wall into the intima in response to environmental stimuli. There, they may adopt different phenotypes, differentiating into osteoblasts-, chondrocytes-, adipocytes-, or foam cell-like cells. The formation of atherosclerotic plaque is characterized by increased production of extracellular matrix by the constituent cells, particularly VSMCs, forming a multimolecular network. This is most evident in the enhanced synthesis of collagen (types I, II, and IV), which contributes to plaque stability and rigidity, while also facilitating the migration and proliferation of various cell types.

According to previous reports, activated FXIII influences the biochemical processes and various functions of cells involved in the structure of the vascular wall in several ways. Based on experiments conducted on Apoe/FXIII-A1 and Apoe/FXIII-A1/TG2 KO mice, FXIII activity is important in maintaining vascular integrity, and bleeding mortality was increased in double and triple KO mice.

The cells forming the vessel wall also express various growth factors, cytokines, and proteases in addition to extracellular matrix components, which function as pro-angiogenic factors. In contrast, they also produce several anti-angiogenic proteins, one of the most important of which is a glycoprotein, the thrombospondin-1 (TSP-1), that also influences the regulation of angiogenesis. The proangiogenic effect is described in more detail below. FXIIIa enhances fibroblast migration, receptor-mediated phagocytosis of monocytes, and participates in the cross-linking of extracellular matrix proteins.

Inbal and colleagues investigated the role of FXIIIa in angiogenesis in several studies. They have found that activated FXIII cross-links $\alpha_V ß_3$ integrin and vascular endothelial growth factor receptor (VEGFR-2) on the surface of endothelial cells. Following the formation of this bond, the receptor becomes activated and initiates signaling pathways, resulting in decreased TSP-1 expression, increased endothelial cell proliferation and migration, and inhibition of apoptosis. TSP-1 is a homotrimeric glycoprotein that can also serve as a substrate for activated FXIII, forming covalent homo-polymers. TSP-1 can be produced by numerous cells involved in inflammation or angiogenesis. It exerts its effects through cell-surface receptors (CD36, CD47), integrins, and extracellular matrix proteins on surrounding cells.

Furthermore, Somodi and colleagues described that macrophage-derived foam cells present in the plaque contain cFXIII and that it is also present in the extracellular space of the plaque in an active form, as they were able to detect the presence of cross-links in the matrix. In this way, cFXIII can be externalized and activated, participating in maintaining the stability of the extracellular matrix, thereby increasing plaque stability. cFXIII entering the plaque may also have an effect on VSMCs. Currently, little is known about the relationship between FXIII and VSMCs, the main components of atherosclerotic plaque.

2.2.3 The role of FXIII in other physiological processes

FXIII plays an important role not only in blood coagulation but also in numerous other physiological processes, where it participates in the stabilization of the extracellular matrix produced by various cells and in cell stimulation processes. Among the extracellular matrix proteins, fibrin, fibronectin, and collagen are good substrates for FXIII. During pregnancy, pFXIII colocalizes with fibrinogen and fibronectin in the Nitabuch layer, providing protection against fibrinolysis in the connective tissue of the placenta. The presence of cFXIII in the intestinal tract is important in trapping bacteria by cross-linking the fibrin network and removing them. In patients with ulcerative colitis, both the number of macrophages polarized via the alternative pathway and the expression of cFXIII produced by them have been observed to be reduced, which may be responsible for the inflammation that has developed. In chronic inflammatory lung disease, bronchoalveolar inflammation, and asthma, connective tissue fibrin deposition increases. cFXIII, produced by bronchoalveolar cells, alveolar macrophages, and dendritic cells, may contribute to the formation of a stable fibrin mesh. In the tumor cell environment, cFXIII produced by tumor-associated macrophages is also responsible for the formation of a stable fibrin network, which protects tumor cells and promotes their proliferation. Recent studies suggest that cFXIII may also play a role in energy metabolism. Elevated F13A1 gene expression was detected in the white adipose tissue of obese individuals. Fibronectin, produced by white adipose tissue, is an important extracellular substrate for FXIIIa, which is essential for cell proliferation, differentiation, and adipose tissue development.

2.3 Balance of hemostasis, coagulation, and fibrinolysis

The purpose of coagulation is to seal vascular injury, form a stable fibrin network, and protect it from premature degradation. In contrast, fibrinolysis is responsible for breaking down the fibrin clot, thereby preventing vessel occlusion. The hemostatic regulatory system ensures the coordinated functioning of these two opposing processes. During the coagulation cascade, large amounts of thrombin are generated, which convert soluble fibrinogen into fibrin monomers by cleaving fibrinopeptides A and B, while simultaneously activating fibrinogen-bound FXIII by removing its activation peptide. Activated FXIII not only cross-links fibrin fibers but also covalently attaches another substrate, α2PI, to the fibrin α-chain, thereby preventing immediate

clot dissolution by plasmin. The main regulatory enzyme of fibrinolysis, plasmin, rapidly cleaves the fibrin network, producing fibrin degradation products. Elevated fibrinogen concentrations and reduced fibrinolytic efficiency in circulation have been described in various clinical studies as risk factors for venous and arterial thrombotic events.

2.4 The key enzyme of fibrinolysis: plasmin

Plasminogen is a glycoprotein of approximately 92 kDa, composed of 791 amino acids, circulating in plasma at a concentration of about 180 μg/mL, and synthesized primarily in the liver. Its activation is mediated by two serine proteases: tissue-type plasminogen activator (t-PA) and urokinase-type plasminogen activator (u-PA), which cleave plasminogen between Arg561 and Val562. In resulting ~90 kDa active serine protease, the plasmin, is primarily responsible for fibrin clot degradation, but also participates in other biological processes such as wound healing and angiogenesis. The heavy chain of human plasminogen contains five loop-like "kringle domains," each consisting of ~80 amino acids linked by three disulfide bonds. These domains contain lysine-binding sites that facilitate plasmin binding to fibrin, cell-surface receptors, and other proteins such as α2-plasmin inhibitor.

2.5 Structure and properties of α2-plasmin inhibitor (α2PI)

α2PI (also known as α2-antiplasmin) is the main physiological inhibitor of plasmin and plays a crucial role in the fibrinolytic system by regulating plasmin activity. Congenital α2PI deficiency causes severe bleeding disorders due to increased susceptibility to fibrinolysis, while elevated plasma levels lead to an increased risk of thrombosis. Moroi and colleagues first mentioned α2PI in 1976, and later, in 1977, Wiman and colleagues successfully isolated it from human plasma. α2PI is a single-chain glycoprotein of ~67 kDa containing 13% carbohydrate. It is produced by hepatocytes and circulates in plasma at ~1 μM concentration, but small amounts have also been detected in the kidney and brain. The human α2PI encoded by the SERPINF2 gene consists of 10 exons and 9 introns, spanning ~16 kilobases of DNA. α2PI is composed of a 27-amino-acid signal peptide and an additional 464 amino acids, belonging to the serine protease inhibitor (serpin) superfamily. It is responsible for the rapid inhibition of plasmin, the key enzyme of fibrinolysis. The complete cDNA sequence shows 23–28% homology with other members of the serpin family. Unlike other serpins, however, the C-terminal end of α2PI is about 50 amino acids longer and

contains numerous lysine amino acids, which interact with the Lys-binding site of plasmin(ogen), thereby increasing the plasmin-inhibitory efficiency of α2PI.

2.6 Heterogeneity of α2PI in plasma

2.6.1 N-terminal modification

In plasma, α2PI undergoes proteolytic cleavage, resulting in four plasma isoforms. The full-length form starting with methionine (Met-α2PI) is cleaved N-terminally between Pro12 and Asn13 by soluble fibroblast-activating protein (sFAP), also known as antiplasmin-cleaving enzyme (APCE), resulting in a 452-amino-acid variant (Asn-α2PI). This form accounts for approximately 70% of total α2PI in normal human plasma. A polymorphism may affect the amino acid at position 6, where a nucleotide substitution (C>T) leads to an amino acid change from arginine (Arg) to tryptophan (Trp). The Arg6Trp polymorphism influences the N-terminal cleavage of Met-α2PI: with Arg6 present, sFAP cleaves the 12-amino-acid peptide eight times faster. As a result of cleavage, FXIIIa has better access to the newly formed N-terminal Gln2 (Gln14, in the full-length form) residue, and the Asn-α2PI variant is cross-linked to fibrin at position K303 about 13 times faster than the full-length form. Plasmin inhibition is not affected by the Arg6Trp polymorphism.

2.6.2 C-terminal modification

In circulation, α2PI can also be modified at the C-terminus, which plays an important role in binding and inhibiting plasmin(ogen). In the intact, non-cleaved form, six lysine residues (K^{418}, K^{427}, K^{434}, K^{441}, K^{448}, K^{464}) are present, enabling binding to plasmin(ogen) (PB-α2PI, plasminogen-binding variant). Although the exact cleavage site is not yet known, the truncated form definitely loses the segment containing the last two lysine residues, which were found to be the most important for plasmin(ogen) binding; therefore, this form is referred to as the non-plasminogen-binding variant (NPB-α2PI). This designation is not entirely accurate, since Clemmensen et al. (1981) reported that α2PI, even after removal of the last 23 amino acids (including K^{448} and K^{464}), can still form a complex with plasmin, although in this case the reaction proceeds ten times more slowly. According to Wang et al., K^{448} plays the most important role in plasmin interaction, while a 2011 study of recombinant α2PI variants found that binding is primarily due to K^{464}, followed by K^{448}. Abdul et al. suggested that the main cleavage site in the C-terminal region is between Gln421

and Asp422, though other potential sites have also been identified. Orosz et al. reported a possible cleavage site between Pro437 and Arg438. The protease(s) responsible for this modification have not yet been identified. Several studies have described in vitro cleavage of PB-α2PI by enzymes such as trypsin, elastase, or matrix metalloproteinase-3 (MMP-3), but whether these proteases are responsible for C-terminal cleavage in vivo remains unproven. In healthy controls, the proportion of NPB-α2PI in plasma has been found to be approximately 35%.

2.7 Functions of α2PI in circulation

The main function of α2PI is to form a stable 1:1 complex with plasmin (PAP complex) either in circulation or on the fibrin surface. The reaction proceeds via a two-step mechanism: first, α2PI interacts non-covalently and reversibly with the kringle domains of plasmin through lysine residues at its C-terminal end. This is followed by an irreversible, first-order reaction in which a covalent bond forms between the reactive site of α2PI and the active site of plasmin. In the PAP complex formed at the end of the process, plasmin loses its activity. α2PI also competitively inhibits plasminogen binding to fibrin. The half-life of the PAP complex circulating in plasma is approximately 12 hours.

2.8 Formation of the fibrin network during coagulation

Fibrinogen is a 340 kDa glycoprotein produced by hepatocytes, present in human plasma at a concentration of 2–4 g/L. Functionally, it is indispensable in hemostasis, wound healing, and angiogenesis. As an acute-phase protein, its plasma level can increase two- to fourfold during inflammatory processes. Structurally, fibrinogen consists of three polypeptide chains (Aα-chain, Bβ-chain, and γ-chain), which are held together by disulfide bonds.

Fibrinogen plays an important role in both primary and secondary hemostasis. During primary hemostasis, the C-terminal ends of the γ-chains bind to the surface of activated platelets, leading to platelet aggregation and the formation of a platelet “plug.” In secondary hemostasis, fibrinogen is converted into fibrin. First, thrombin cleaves two fibrinopeptides (A and B) from the N-terminal ends of the Aα and Bβ chains, generating fibrin monomers. These monomers undergo spontaneous polymerization, which does not require enzymatic catalysis. The next phase is fibrin stabilization, during which FXIIIa forms a covalent cross-link between fibrin γ-chains and α-chains.

During blood coagulation, numerous proteins can bind to the fibrin network, thereby influencing its structure and resistance to fibrinolysis. Wiesel summarized these macromolecules in his publication, including fibronectin, plasminogen, coagulation factor XIII, tissue plasminogen activator (t-PA), plasminogen activator inhibitor-1 (PAI-1), actin, albumin, α1-antitrypsin, carboxypeptidase-N, lipoprotein(a), and TSP-1.

In a 1981 *in vitro* experiment, it was demonstrated that α2PI is not fully incorporated into the clot but only by approximately 30%, whereas Katona and colleagues in their 2021 publication estimated incorporation at about 45%. The covalent incorporation of α2PI into the clot is due to FXIIIa. Several glutamine residues have been identified (Gln^{2}, Gln^{21}, Gln^{419}, and Gln^{447}) as potential substrates for the enzyme, although the main reactive site is the N-terminally located Gln^{2}. Currently, very little reliable knowledge is available regarding the incorporation of C-terminal α2PI forms into the fibrin network. The main reason is that, due to the lack of suitable methods, the extent of incorporation is difficult to quantify, and the nature of binding is also difficult to identify. Kluft and colleagues, investigating C-terminal variants, found that the primary form incorporated into fibrin clots is PB-α2PI, and FXIIIa is responsible for this incorporation. Since, in the absence of FXIII—that is, without covalent cross-linking—fibrinolysis is enhanced, non-covalent binding of α2PI to fibrin fibers was not considered significant and therefore was not studied extensively. However, Tsurupa and colleagues demonstrated that α2PI non-covalently binds to fibrin and immobilized fibrinogen, and that this binding cannot be inhibited by lysine analogs, indicating that the C-terminally lysine-binding region does not participate in this process. It was hypothesized that the non-covalent interaction promotes the formation of cross-links by FXIIIa.

3. OBJECTIVES

In the present study, we sought answers to the following questions:

1. Does the osteoblastic transformation of HAoSMCs involve cellular FXIII expression?
2. Does FXIIIa influence the proliferation, migration, and collagen secretion of HAoSMC?
3. Does FXIIIa affect the synthesis of TSP-1 in HAoSMCs, as well as their intracellular and cell-associated TSP-1 content?
4. Which parameters are associated with the plasma levels of the C-terminal isoforms of α2-plasmin inhibitor and with the extent of their incorporation into the fibrin clot?
5. What is the relationship between the incorporation of PB- and NPB-α2PI forms into the clot and clot lysis parameters in healthy human plasma samples?
6. Can it also be confirmed that the results obtained with normal plasmas by using α2PI-deficient plasma supplemented with recombinant PB and NPB α2PI forms? How do the different forms influence clot lysis and the structure of the resulting clot?

4. MATERIALS AND METHODS

4.1 Materials I.

Recombinant FXIII-A_2 (rFXIII-A_2) is provided by Novo Nordisk (Malmö, Netherlands). In the experiments, we used FXIII-A_2-depleted fetal calf serum, in which only very low concentrations of the FXIII-A subunit were detectable. In medium containing 5% FBS, the concentration was 19.75 ng/mL, corresponding to 0.2% of plasma FXIII-A levels. To remove the FXIII-A_2 subunit from the serum, an immunoabsorption chromatographic technique was used. For this purpose, a mouse-derived monoclonal antibody against FXIII-A_2 (3B2H12) was used. The antibody was covalently bound to the surface of CNBr-activated Sepharose 4B gel (GE Healthcare Bio-Sciences AB, Uppsala, Sweden).

4.2 Cell culture

Human aortic smooth muscle cells (HAoSMC, Cell Applications, San Diego, CA, USA) were used in the experiments. Cells were cultured in high-glucose Dulbecco's Modified Eagle Medium (DMEM, Sigma Aldrich, St. Louis, MO, USA). The medium was supplemented with 1 mM sodium pyruvate (Sigma Aldrich, St. Louis, MO, USA), 4 mM L-glutamine (Sigma Aldrich, St. Louis, MO, USA), 116 µg/mL gentamicin (Sandoz Hungária Kft., Budapest, Hungary), and 5% FBS (Thermo Fisher Scientific, Waltham, MA, USA). The medium was replaced every other day, and cells were used from passages 5-9.

4.3 Effect of osteoblastic transformation on HAoSMCs

To induce osteoblastic transformation, HAoSMCs were cultured in a 6-well plate using calcification medium. The medium was supplemented with 2.5 mM inorganic phosphate (Pi), 1.2 mM Ca^{2+}, and 3% FBS. Cells maintained in culture medium were used as controls. At 80% confluence, after 24 hours, the culture medium was replaced with calcification medium. Two days later, the medium was changed, and after 48 hours, the expression of osteoblastic differentiation markers was determined according to the manufacturer's instructions.

1. Calcium deposition was quantified using the QuantiChrome Calcium Assay Kit (Gentaur, DICA:500, Brussels, Belgium). Absorbance was measured at 612 nm using a spectrophotometer (Powerwave XS, Bio-Tek).

2. Calcium deposition in the extracellular matrix was visualized by Alizarin Red staining. To dissolve the dye, cells were incubated for 1 hour at room temperature with 1 mL/well of 100 mM cetylpyridinium solution. Absorbance was measured at 595 nm using a spectrophotometer (Beckman Coulter DTX 880 Multimode Detector).

3. Osteocalcin content in the extracellular matrix was determined by ELISA (Human Osteocalcin Instant ELISA, Bender MedSystems 2020, Burlingame, CA, USA). Absorbance was measured at 450 nm using an ELISA Reader (Beckman Coulter DTX 880 Multimode Detector).

4. Alkaline phosphatase (ALP) activity was measured from cell lysates using the ALP Yellow Liquid Substrate kit (Sigma Aldrich, St. Louis, MO, USA). Enzyme release was determined based on the amount of 4-nitrophenol at 405 nm for 30 minutes at 37 °C.

5. Runx2 gene expression was determined by quantitative real-time PCR (qRT-PCR). RNA isolation was performed according to the manufacturer's protocol (RNA-STAT60, Tel-Test Inc., Friendswood, Texas, USA). Using the High-Capacity cDNA RT kit (Applied Biosystems, Thermo Fisher Scientific, Waltham, MA, USA), 2 µg of RNA was reverse-transcribed into cDNA. Amplification of the Runx2 gene was performed with TaqMan primer Hs535845 (Life Technologies, Waltham, MA, USA). GAPDH was used as a housekeeping gene. Relative gene expression changes were calculated using the delta-delta (ΔΔCt) method.

6. Detection of intracellular osteocalcin and Runx2 proteins was performed by Western blot analysis. GAPDH was used as a housekeeping control. Cell lysates containing 15 µg of total protein were prepared in Laemmli buffer with β-mercaptoethanol and denatured at 95 °C. Proteins were separated on 10% SDS-polyacrylamide gels and transferred to nitrocellulose membranes (Amersham, Buckinghamshire, UK) using a semi-dry blotting system (Bio-Rad, Hercules, CA, USA). Membranes were blocked with 6% milk powder, then incubated with primary antibodies: polyclonal anti-osteocalcin (Santa Cruz Biotechnology, Santa Cruz, CA, in 1:200 dilution), rabbit anti-Runx2 (Proteintech, Manchester, UK, in 1:1000 dilution), and mouse anti-GAPDH (Novus Biologicals, Abingdon, UK, in 1:1000 dilution). Secondary antibodies conjugated with horseradish peroxidase (Amersham, Buckinghamshire, UK) were used. Detection was performed with chemiluminescent substrate (ECL, Bio-Rad, Hercules, CA, USA), and a light-sensitive film was used for visualization (Amersham Hyperfilm ECL, GE Healthcare, Buckinghamshire, UK).

7. Cellular cFXIII concentration was determined by ELISA. Streptavidin-coated ELISA plates (Kaviogen, Turku, Finland) were used. Biotinylated monoclonal anti-FXIII-A antibody (1

µg/mL) and HRPO-conjugated anti-FXIII-A antibody (in 1:2000 dilution) were applied. Detection was performed using TMB substrate (One Component HRP Microplate Substrate, Diarect Ag, Freiburg, Germany), and the reaction was stopped with 2 M sulfuric acid.

8. Expression of cellular cFXIII was also determined by Western blot. A 10% SDS-polyacrylamide gel was used. Recombinant FXIII-A_2 standard (Novo Nordisk, 10 ng) and 30 µg of total protein per sample were loaded. Proteins were transferred to PVDF membranes (Bio-Rad, Hercules, CA, USA) using a semi-dry blotting system. Membranes were blocked with tTBS buffer containing 3% gelatin (pH 7.5). For the primary antibody, sheep polyclonal anti-FXIII-A (Affinity Biologicals, ON, Canada; in 1:5000 dilution), and for the secondary antibody, biotinylated anti-sheep IgG (Vectastain ABC Kit, Vector Laboratories, Oxfordshire, UK; in 1:10.000 dilution) were used. After the addition of avidin-biotin HRPO complex (Vectastain ABC Kit, PK6106; in 1:3200 dilution), for detection, a chemiluminescent substrate (Covalab, Cambridge, UK), and for visualization, a light-sensitive film (Amersham Hyperfilm ECL, Buckinghamshire, UK) was used.

4.4 Treatment of HAoSMCs with activated and non-activated rFXIII

As a first step, we prepared a stock solution containing 20 µg/mL rFXIII-A_2 in DMEM medium containing 0.2% FXIII-A_2-free FBS. In the next step, FXIII-A_2 was activated (rFXIIIa) with 5 U/mL human thrombin and 1 mM $CaCl_2$ for 10 minutes at 37 °C. Subsequently, the thrombin was antagonized with 50 ATU/mL lepirudin derivative (Refludan; Pharmion, Windsor, UK) for 10 minutes at 37 °C. Further dilutions were prepared from the stock solution (15, 10, 5, and 2.5 µg/mL rFXIIIa). The diluent solution required for the dilutions contained 1 mM $CaCl_2$, 5 U/mL human thrombin inhibited with 50 ATU/mL Refludan, and 0.2% FXIII-A_2-depleted FBS. For treatment with non-activated rFXIII-A_2, we prepared dilutions with final concentrations of 15, 10, 5, and 2.5 µg/mL from a 20 µg/mL rFXIII-A_2 stock solution in culture medium containing 0.2% FXIII-A_2-depleted FBS.

At 24 hours after distribution, the culture media were replaced with media containing activated or non-activated FXIII-A. Since thrombin alone can increase cell proliferation, we used a medium containing 5 U/mL human thrombin inhibited with 50 ATU/mL Refludan and 1 mM $CaCl_2$ as a control. The treatments were carried out for 1 or 3 days.

4.5 Execution of the cell proliferation assay

HAoSMCs were seeded into 96-well plates (TPP Techno Plastic Products AG, Switzerland) at 0.6×10^4 cells/well. For seeding, DMEM medium containing 5% FBS was used. Treatments were started 24 hours after plating. Dilutions of activated and non-activated 20 µg/mL rFXIII stock solution were prepared to final concentrations of 15, 10, 5, and 2.5 µg/mL. The control cells were cultured in a medium containing thrombin inhibited with Refludan. Treatments were repeated every 24 hours for three days. Cell proliferation was determined 24 hours after the final treatment using the EZ4U Cell Proliferation and Cytotoxicity Assay (Biomedica, Vienna, Austria) and the CCK-8 Cell Counting Kit (Enzo Life Sciences, Farmingdale, NY, USA), according to the manufacturers' instructions. Both assays are based on the principle that mitochondrial dehydrogenase enzymes in viable cells reduce yellow tetrazolium salts to dark-colored formazan. The color change was detected spectrophotometrically (iEMSReader MF and Multiscan™) at 450 nm after 4 hours of incubation at 37 °C. Absorbance values were directly proportional to the number of viable cells.

4.6 Detection of cell migration

The CytoSelect 24-Well Wound Healing Assay (Cell Biolabs, San Diego, CA, USA) kit includes a 24-well tissue culture plate containing specific inserts that prevent cell attachment in defined areas. HAoSMCs were seeded into wells containing inserts at 20×10^4 cells/well in DMEM medium supplemented with 5% FBS. The control cells were cultured in a medium containing thrombin inhibited with Refludan. Treatments were started 24 hours after plating, performed in duplicate wells with final concentrations of rFXIIIa at 20, 15, 10, 5, and 2.5 µg/mL. After 24 hours of treatment, inserts were removed, and wound gap closure was recorded using the Juli Stage Real-Time Cell History Recorder Microscope (NanoEnTek, Seoul, South Korea) in a CO_2 incubator. Three different positions in each well and three parallel wells were analyzed for each treatment.

4.7 Determination of collagen content in the extracellular matrix

HAoSMCs were seeded into 12-well tissue culture plates (TPP) at 10×10^4 cells/well. Treatments were started 24 hours after plating and continued for 3 days with rFXIIIa at final concentrations of 20, 15, 10, 5, and 2.5 µg/mL. The control cells were cultured in a medium containing thrombin

inhibited with Refludan. Twenty-four hours after the final treatment, collagen content in the extracellular matrix was measured using the Sircol™ Soluble Collagen Assay Kit (Biocolor Life Science Assays, Carrickfergus, UK), according to the manufacturer's instructions. Following dissolution of the collagen-dye complex, absorbance was detected at 450 nm using a spectrophotometer (iEMSReader MF and Multiscan™), and results were evaluated with Ascent software.

4.8 Determination of TSP-1 from cell fraction and cell supernatant

HAoSMCs were seeded into 96-well tissue culture plates (TPP) at 0.6×10^4 cells/well. Treatments were initiated 24 hours after plating and lasted for 24 hours. Dilutions of 20 µg/mL rFXIIIa stock solution were prepared to final concentrations of 15, 10, 5, and 2.5 µg/mL. The control cells were cultured in a medium containing thrombin inhibited with Refludan. The following day, supernatants (200 µL/well) were removed, and cells were washed with PBS buffer (200 µL/well). Cell lysates were prepared by adding PBS buffer (200 µL/well) containing 1% Triton X-100, 1 mM EDTA, and 10% protease inhibitor cocktail (SigmaFast, Sigma Aldrich, St. Louis, MO, USA). Incubation was performed for 5 minutes with gentle shaking, followed by mixing and centrifugation at 13400 rpm for 5 minutes. Supernatants were transferred into low-protein-binding tubes. TSP-1 protein levels were determined using the Human Thrombospondin 1 ELISA kit (Thermo Fisher Scientific, Waltham, MA, USA), according to the manufacturer's instructions. Absorbance was measured at 450 nm (iEMSReader MF and Multiscan™ photometer), and results were analyzed using Ascent software.

4.9 Investigation of TSP-1 protein production in HAoSMCs cells by Western blot

HAoSMCs were seeded into 6-well tissue culture plates (TPP) at 50×10^4 cells/well. Treatments with 20 µg/mL rFXIIIa were started 24 hours after plating for 24 hours. The control cells were cultured in a medium containing thrombin inhibited with Refludan. Cells were washed with PBS buffer (1500 µL/well) containing 2 mM EDTA and 10% protease inhibitor (Biotool, Houston, USA) for 30 minutes at 37 °C. Cells were collected from the plate surface and centrifuged at 13200 rpm. Cell pellets were lysed with RIPA buffer (0.1% SDS, 0.5% deoxycholate, 1% Triton X-100). The extracellular matrix remaining on the culture plate was washed with PBS buffer containing 2 mM EDTA and 10% protease inhibitor cocktail. Wells were then incubated with 500 µL Laemmli

buffer at room temperature with shaking (150 rpm) for 30 minutes. Samples containing extracellular matrix proteins were collected and concentrated using 10 kDa Microcon filters (YM-10, Millipore, Sigma Aldrich, St. Louis, MO, USA). Total protein content was determined from both cell pellets and matrix samples using a BCA kit (Thermo Fisher Scientific, Waltham, MA, USA). Protein separation was performed on 7.5% SDS-polyacrylamide gels. Samples included 200 ng TSP-1 standard (Thrombospondin Human Platelet, Athens Research and Technologies, Athens, Georgia, USA), 54 µg total protein from cell lysates, and 2 µg total protein from extracellular matrix samples. Proteins were transferred to PVDF membranes (Bio-Rad, Hercules, CA, USA) using a semi-dry blotting system (Bio-Rad, Hercules, CA, USA). Membranes were blocked with tTBS buffer (150 mM NaCl, 50 mM Tris, 0.05% Tween-20, pH 7.5) containing 3% BSA (Sigma Aldrich, St. Louis, MO, USA) for 2 hours. For the primary antibody, mouse-derived biotinylated monoclonal anti-thrombospondin-1 (Life Technologies; 1:1000 dilution), and for the secondary antibody, HRPO-conjugated polyclonal goat anti-mouse IgG (Bio-Rad, Hercules, CA, USA; 1:20000 dilution) were used. For detection, a chemiluminescent substrate reagent (ECL, Bio-Rad, Hercules, CA, USA) and for visualization, a light-sensitive film (Amersham Hyperfilm ECL, Buckinghamshire, UK) were used.

4.10 Detection of TSP-1 protein by immunofluorescent staining

HAoSMCs were seeded into Clipmax 10 cm² culture flasks (Techno Plastic Products AG, Trasadingen, Switzerland) at 8×10^4 cells/flask. The side of the flask can be removed, and the bottom serves as a microscope slide. Twenty-four hours after plating, cells were treated with 20 µg/mL rFXIIIa; control cells were cultured in medium containing thrombin inhibited with Refludan. After 24 hours, cells were washed with PBS buffer and fixed for 10 minutes with 96% ethanol containing 3% acetic acid. Following another PBS wash, blocking was performed with 5% normal human serum for 15 minutes. For immunofluorescent staining, biotinylated mouse monoclonal anti-TSP-1 antibody (Thermo Fisher Scientific, Waltham, MA, USA, 1:200 dilution) was applied for 60 minutes, followed by DyLight 488-conjugated horse anti-mouse IgG antibody (Vector Laboratories, Oxfordshire, UK, 1:100 dilution) for 45 minutes. Cell nuclei were stained with 4′,6-diamidino-2-phenylindole (DAPI, Vectashield Antifade Mounting Medium with DAPI, Vector Laboratories, Oxfordshire, UK). Slides were examined with an AxioImage.M2

fluorescence microscope (Zeiss, Oberkochen, Germany), and representative images were acquired by confocal laser scanning microscope (LSM 700, Zeiss, Oberkochen, Germany).

4.11 Investigation of TSP-1 gene expression

HAoSMCs were seeded into 24-well plates (TPP) at 3×10^4 cells/well. Twenty-four hours after seeding, cells were treated with rFXIIIa at final concentrations of 20, 15, 10, 5, and 2.5 µg/mL. The control cells were cultured in a medium containing thrombin inhibited with Refludan. After 24 hours of treatment, total RNA was isolated from the cultures using the QIAamp RNA Blood Mini Kit (Qiagen, Hilden, Germany), according to the manufacturer's instructions. RNA concentration and purity were determined with a NanoDrop2000 spectrophotometer (Thermo Fisher Scientific, Waltham, MA, USA). cDNA synthesis was performed using the qPCR BIO cDNA Synthesis Kit (PCR Biosystems, London, UK), with 80 ng RNA reverse-transcribed into cDNA. The reaction was carried out on a Veriti 96-well Thermal Cycler PCR system. Quantitative real-time PCR was performed to amplify the TSP-1 gene, and GAPDH was used as a housekeeping gene. Primer sequences matched those published by Dardik et al. PCR reactions were carried out on a LightCycler 480 instrument (Roche, Budapest, Hungary) using LightCycler 480 SYBR Green I Master Mix (Roche, Budapest, Hungary). Gene expression levels were calculated using the ΔΔCt method, normalized to GAPDH.

4.12 Human samples

Eighty plasma samples from healthy individuals were randomly selected from the sample pool of our previous study. All chronic diseases except for moderate hypertension (blood pressure between 145/90 and 165/95 mmHg) and any acute illness in the previous 3 weeks were considered as exclusion criteria for healthy controls. Blood was taken from the antecubital vein into vacutainer tubes (Beckton Dickinson, Franklin Lakes, NJ, USA) containing 1/10 volume of 0.109 M citrate between 8 am and 11 am. Plasma was separated by centrifugation at 1500 × g for 20 minutes and aliquots were stored at –70 °C until measurements. All enrolled individuals gave written informed consent. The study fully complied with the Declaration of Helsinki. Ethical approval was obtained from the Regional Ethics Committee at the University of Debrecen, Hungary (ETT TUKEB: 54005-3/2016/EKU).

4.13 Materials II.

All forms of α2PI were isolated using affinity chromatography with the same monoclonal anti-α2PI antibody as used in the total-α2PI ELISA assay from plasma samples. From the α2PI preparation, the PB-α2PI form was further separated by an additional affinity chromatography step using a plasminogen-Sepharose column. In this way, the preparation retained the non-plasminogen-binding NPB-α2PI form. Recombinant α2PI proteins were purchased from Sino Biological (Beijing, China): full-length α2PI (Human Serpin F2 Protein, Met-PB-α2PI, 1–464 aa) and C-terminally truncated α2PI (Human Serpin F2 Protein, Met-NPB-α2PI, 1–437 aa). α2PI-deficient plasma was obtained from Affinity Biologicals (ON, Canada). Human plasma-derived thrombin was purchased from Sigma Aldrich (St. Louis, MO, USA). Human tissue factor was obtained from Innovin (Siemens, Marburg, Germany), and recombinant t-PA from Actilyse (Boehringer Ingelheim International, Germany) was used in various experiments. Human plasma-derived fibrinogen (Sigma Aldrich, St. Louis, MO, USA) was labeled with Alexa-Fluor647 dye (Life Technologies, Waltham, MA, USA) according to the manufacturer's protocol.

4.14 Determination of α2-plasmin inhibitor concentration in plasma samples

The total-α2PI antigen concentration was measured by an in-house sandwich ELISA, as previously described. This assay measures all plasmatic forms of α2PI and is not influenced by the presence of plasmin–antiplasmin complexes (reference range of plasma α2PI: 48–85 mg/L). PB-α2PI antigen concentration was also measured by using a sandwich ELISA developed by our research group. The amount of NPB-α2PI was calculated by subtraction of the PB-α2PI concentration from the total α2PI concentration.

4.15 Investigation of α2PI incorporation into plasma clots

Plasma samples were clotted by adding 2 U/mL thrombin and 20 mM $CaCl_2$ (activation mix) for 30 minutes at 37 °C. Serum was separated from the clot by centrifugation (16100 × g, 5 minutes). Total, PB-, and NPB-α2PI antigen levels were measured from the original plasma samples and the obtained serum using the ELISA techniques described above. Values measured in the serum were multiplied by the dilution factor (1.11) caused by the addition of the coagulation activation mix. Incorporated α2PI forms were calculated by subtracting the amount of α2PI measured in the serum

from the corresponding value measured in the plasma. α2PI incorporation into the clot was also investigated by Western blot. Three randomly selected samples were clotted as above in the presence or absence of 2 mM iodoacetamide (IAA). After intensive washing with PBS (pH 7.2) containing 3 mg/mL IAA, clots were dissolved in Laemmli buffer containing 5% mercaptoethanol and 8 M urea at room temperature for 20 h and analyzed by SDS-PAGE on 7.5% polyacrylamide gels. Human plasma-purified α2PI preparation (Calbiochem, San Diego, CA, USA) was used as a standard. Proteins were transferred to PVDF membranes (Bio-Rad, Hercules, CA, USA) using the Trans-Blot Turbo Transfer System (Bio-Rad, Hercules, CA, USA). Membranes were blocked for 1 hour at room temperature with TBS (pH 7.4) containing 3% gelatin. Between incubation steps, membranes were washed three times for 5 minutes with tTBS (pH 7.4). For the detection of all isoforms, HRPO-conjugated polyclonal anti-human α2PI antibody (GA2AP-AP, Affinity Biologicals, ON, Canada, 1:20000 dilution) was used. For detection of the PB-α2PI form, mouse monoclonal anti-human PB-α2PI antibody (Monoclonal anti-α2AP 3AP, Technoclone, Vienna, Austria) was used at 3 µg/mL, followed by HRPO-conjugated anti-mouse IgG antibody (Southern Biotech, Birmingham, AL, USA, 1:3000 dilution). ECL chemiluminescent reagent (Thermo Fisher Scientific, Waltham, MA, USA) for detection, and an Azure Biosystems c300 instrument (Azure Biosystems, Dublin, CA, USA) for visualization were used.

4.16 Fibrin clot lysis assays

An *in vitro* fibrin clot lysis assay was performed on 80 healthy plasma samples, as described in the method of Orbán-Kálmándi et al. To investigate the effect of recombinant full-length and C-terminally truncated α2PI on clot lysis, we applied a modified clot lysis time determination. α2PI-deficient plasma was supplemented with different forms (full-length and C-terminally truncated) of recombinant α2PI proteins, with 65 µg/mL plasma concentration defined as 100%. The plasma mix contained 1.3-fold diluted plasma, Innovin diluted in HEPES buffer (1:100, pH 7.4), and 130 ng/mL rt-PA. To initiate clotting, an activation mix containing 1 U/mL thrombin and 1 mM $CaCl_2$ in HEPES buffer was added. For each well of a 96-well plate (Greiner Bio-One, Kremsmünster, Austria), 50 µL plasma mix was combined with 25 µL activation mix. Turbidity was immediately measured at 340 nm every minute for 72 minutes at 37 °C using a Tecan Infinite 200 spectrophotometer (TECAN Trading AG, Männedorf, Switzerland). Shiny App software (Simple clot lysis analysis app version 0.3.1) was used to fit the turbidimetry curves of fibrin formation

and lysis and determine different parameters of the curve, such as the maximum clot amplitude/absorbance (MaxAbs), 50% clot lysis time (CLT50, the difference between the time required to reach 50% maximum absorbance on the ascending branch of the lysis curve and the time required to reach 50% lysis), and the area under the curve (AUC).

4.17 Examination of clot structure by confocal laser scanning microscopy

α2-antiplasmin-deficient plasma was supplemented with different amounts of recombinant full-length and/or C-terminally truncated α2PI forms were also substituted with AF647-labeled fibrinogen to obtain a 2% labeled fibrinogen fraction. Clot formation was induced by adding 50 µL activation mix containing 0.5 U/mL thrombin and 10 mM CaCl2 in TRIS/HCl buffer (pH 7.5) to 50 µL plasma. Forty µL samples were loaded immediately into channels of an Ibidi µ-Slide VI and incubated in the dark for two hours at room temperature in a wet chamber. Wells on both sides of the channel were filled with TRIS/HCl buffer. On one side, a 2.5 mL syringe was plugged into the well and filled up with TRIS/HCl buffer to 2 mL. Clots were washed for 2 hours and investigated with an Olympus FluoView 3000 confocal microscope (Olympus, Tokyo, Japan). The total thickness of the Z-stack measured 42 µm, with a Z-stack size of 2.0 µm, resulting in a total of 22 Z-slices. For confocal image analysis of the clot structures, an open-source software, Fiji (version 2.3, Fiji Is Just ImageJ), was used. To determine the pore size of the clots, the average radius of bubbles that can fit into the 2D pores and produce maximum coverage of the entire 2D image was calculated; the procedure employed was based on the source code developed by Munster et al. The fiber width was calculated using a MATLAB (R2019a) GUI called CT-FIRE v3.0 beta (Curvelet Transform—Fiber Extraction). Twenty-two images (1024 × 1024 pixels) of each slide were recorded in the same positions in a Z-stack. Different parameters (% area covered, pore-size (average radius of bubbles), fiber width) were calculated from the 22 evaluated images and expressed as mean ± SD.

4.18 Other laboratory methods

FXIII activity was measured by an ammonia release assay using the Technochrom FXIII chromogenic assay (Technoclone, Vienna, Austria). FXIII-A_2B_2 antigen levels were measured by sandwich ELISA as previously described. Fibrinogen concentration was measured using the Clauss method. Plasminogen was measured using the Berichrom Plasminogen assay (Siemens Healthcare

Diagnostics GmbH, Marburg, Germany) on a BCS XP coagulometer (Siemens Healthineers, Erlangen, Germany).

4.19 Statistical analysis

In the results obtained from experiments with HAoSMCs, Student's t-test was used to assess statistical significance, and $p < 0.05$ was considered statistically significant. Means represent the results of at least 6 individual measurements. In the results obtained from experiments with α2PI, a correlation sample size calculator was used to calculate the required sample size. The required sample size is N = 80 to establish a statistically significant correlation of $r > 0.300$ at alpha = 0.05 and beta = 0.2. The Kolmogorov–Smirnov test was used for the distribution of the data. Data are presented as mean ± SD or median (interquartile range) depending on the distribution. To investigate the correlation of α2PI levels with the incorporation of different α2PI forms into the plasma clot and different clot lysis parameters, bivariate (Pearson) correlation analyses were performed. For this analysis, non-normally distributed variables were naturally log-transformed to achieve normal distribution. An independent sample t-test was used to test differences in means of different clot lysis and clot structure parameters of plasma samples supplemented with recombinant α2PI. The level of significance was 95% ($p < 0.05$). Statistical analyses were performed using SPSS software (SPSS 28.0 for Macintosh, Chicago, IL, USA).

5. RESULTS

5.1 Effects of activated FXIII on HAoSMCs

5.1.1 FXIII-A expression during osteoblastic transformation of HAoSMCs

Since FXIII-A is also found in human osteoblast cells, we first wanted to investigate whether the osteoblastic transformation of HAoSMCs is associated with FXIII-A expression. To achieve osteoblastic differentiation, cells were cultured in calcification medium containing 2.5 mM inorganic phosphate (Pi) and 1.2 mM Ca2+. The calcium content detected by Alizarin Red S staining was elevated in the transformed cells compared to the control cells (17.34±3.2 vs. 204.42±13.8). Osteocalcin (OCN) synthesis increased 9-fold compared to the control (6.34±1.0 vs. 58.42±7.8), and Runx2 gene expression increased 1.69-fold compared to the control. Alkaline phosphatase activity in the transformed cells increased 8.67-fold compared to the control cells. The increase in the levels of these markers confirmed that osteoblastic transformation had occurred. Nevertheless, FXIII-A was not detectable in the cell lysates by either Western blot or ELISA techniques.

5.1.2 The effect of rFXIII-A_2 on HAoSMC proliferation

Next, we investigated the effect of externally added rFXIII-A_2 on HAoSMCs. The extracellular concentration of FXIII-A in hemorrhagic plaques is unknown, but it is presumably higher than the plasma concentration (10 µg/mL). Therefore, in our experiments, we applied recombinant FXIII-A in the 2.5–20 µg/mL range. Non-activated rFXIII-A_2 did not affect HAoSMC proliferation, even at the highest applied concentration. In contrast, recombinant activated FXIII-A (rFXIIIa) significantly enhanced cell proliferation in a concentration-dependent manner compared to the control. The increase was already significant below plasma concentration, and the highest applied concentration (20 µg/mL) resulted in a 44% enhancement of proliferation. Cell proliferation was assessed using both EZ4U and CCK-8 kits, which yielded similar results.

5.1.3 The role of rFXIIIa in *in vitro* wound healing

Next, we investigated the effect of rFXIIIa in an *in vitro* wound closure assay. In this experiment, cell proliferation and migration occur simultaneously as cells grow into the empty area. Wound closure can be monitored kinetically. Since our proliferation experiments showed that non-

activated FXIII-A did not influence HAoSMC proliferation, in the following assays, we used only its activated form. Our results demonstrated that rFXIIIa enhanced wound closure in a concentration-dependent manner. Cells treated with 5 µg/mL rFXIIIa reached 30% and 80% confluence at 143 and 581 minutes, respectively; at 10 µg/mL at 98 and 462 minutes; at 15 µg/mL at 82 and 321 minutes; and at 20 µg/mL at 38 and 193 minutes. In contrast, control cells required more time to reach these levels of confluence (192 and 636 minutes).

5.1.4 Collagen secretion by HAoSMCs

Collagen, a key component of the extracellular matrix, was measured after three days of treatment. At 24 hours following the last treatment, collagen levels in the extracellular matrix increased: by 10% with 10 µg/mL rFXIIIa, by nearly 30% with 15 µg/mL, and by 50% with 20 µg/mL compared to untreated cultures.

5.1.5 Detection of TSP-1 in culture medium and cell-associated form

After 24 hours of treatment with rFXIIIa, TSP-1 concentration in the culture medium was significantly reduced compared to control cells: to 78% at 2.5 µg/mL, 54% at 5 µg/mL, 43% at 10 µg/mL, 39% at 15 µg/mL, and 34% at 20 µg/mL. In contrast, TSP-1 concentration in cell lysates increased by 20% at 2.5 µg/mL, 50% at 5 µg/mL, 71% at 10 µg/mL, 100% at 15 µg/mL, and 157% at 20 µg/mL. The total TSP-1 content of each culture was calculated, defined as the sum of TSP-1 measured in the medium and in the cells/cell-associated fraction. Even at the highest rFXIIIa concentration, only a minimal, non-significant decrease was observed in treated cultures compared to untreated ones (135.4 ± 11.4 ng/well vs. 153.1 ± 13.1 ng/well).

5.1.6 Expression of TSP-1 in the cytoplasm of cells

In immunofluorescence analysis, TSP-1 protein was detected only in the cytoplasm of control cells, whereas in the presence of rFXIIIa, numerous small, intensely TSP-1–positive granules were observed, most of which were associated with HAoSMCs.

5.1.7 Detection of TSP-1 by Western blot

Cellular and cell-associated TSP-1 proteins appeared in a high-molecular-weight homotrimer form with strong disulfide bonds in Western blot analysis following reducing SDS-PAGE, compared to the 150 kDa monomeric TSP-1 standard. Densitometric analysis revealed a 2.5-fold increase in cell-associated TSP-1 in rFXIIIa-treated samples compared to control. No TSP-1 was detectable in the extracellular matrix. These findings suggest that treatment with rFXIIIa does not induce *de novo* synthesis of TSP-1, but rather promotes its retention in cell-associated form.

5.1.8 Analysis of TSP-1 mRNA expression

Treatment with rFXIIIa for 24 hours had no significant effect on TSP-1 gene expression in HAoSMCs compared to control cells.

5.2 Results of investigating the impact of α2PI heterogeneity

The consequences of C-terminal cleavage of α2PI in the regulation of fibrinolysis have been less thoroughly studied. In our work, we aimed to investigate how the different α2PI forms and their relative ratios influence plasma clot structure and lysis.

5.2.1 Plasma concentrations of various parameters in the studied population

From a sample collection of healthy individuals gathered for a previous study, we randomly selected 80 plasma samples. All measured parameters were within the reference range. A strong correlation was found between FXIII activity and antigen concentration (r=0.928; $p<0.001$). α2PI activity showed good correlation both with total α2PI antigen concentration (r=0.691; $p<0.001$) and with PB-α2PI antigen concentration (r=0.750; $p<0.001$). However, the correlation between α2PI activity and NPB-α2PI antigen concentration was moderate (r=0.325; $p=0.005$).

5.2.2 Incorporation of α2PI forms into fibrin clots

After clotting the plasma samples, we determined the amounts of total-, PB-, and NPB-α2PI incorporated into the fibrin clots. Following separation of serum and fibrin clots, 44.33 ± 6.3% of total α2PI was incorporated into the clot, of which 57.8% was the PB-α2PI form. Relative to the

original plasma concentration, a greater proportion of NPB-α2PI was incorporated into the clot than PB-α2PI (58.07% vs. 37.62%). Incorporation of PB-α2PI showed significant correlation with FXIII activity (r=0.540; $p<0.001$), fibrinogen (r=0.387; $p<0.001$), and plasminogen concentration (r=0.407; $p<0.001$). In contrast, incorporation of NPB-α2PI did not correlate significantly with FXIII activity (r=0.110; $p=0.331$) or fibrinogen concentration (r=0.086; $p=0.446$), but did correlate with plasminogen levels (r=0.322; $p=0.004$).

5.2.3 Association of measured parameters with clot lysis

Clot lysis assays were performed on the same plasma samples (n = 80), and we examined relationships between the measured parameters and characteristics of the turbidimetric lysis curves (CLT50, MaxAbs, and AUC). Increases in FXIII antigen and activity had a positive effect on MaxAbs and AUC, but not on CLT50. Fibrinogen levels correlated only with MaxAbs. Total α2PI plasma concentration showed statistically significant positive correlation with all three lysis curve parameters; however, for α2PI C-terminal forms, this association was observed only for NPB-α2PI. The plasma PB-α2PI/NPB-α2PI ratio showed a significant negative correlation with both CLT50 and AUC. Interestingly, while both plasma NPB-α2PI and incorporated NPB-α2PI antigen concentrations showed significant positive correlations with CLT50, MaxAbs, and AUC values, for PB-α2PI, only the clot-incorporated form correlated, and only with MaxAbs.

5.2.4 Investigation of α2PI incorporation into fibrin clots by Western blot

To investigate how different α2PI forms are incorporated into fibrin clots, three randomly selected normal human plasma samples were clotted by adding thrombin and Ca^{2+}, either in the presence or absence of the FXIII inhibitor iodoacetamide (IAA). Clots were extensively washed, dissolved, and analyzed by Western blot. A polyclonal anti-α2PI antibody was used to detect all α2PI forms incorporated into the fibrin clot, while a specific monoclonal antibody was applied to determine the localization of the PB-α2PI form. α2PI cross-linked to fibrin α-chains and α-polymers was visible with both antibodies, whereas monomeric α2PI (non-covalently bound) was detected only with the polyclonal antibody. In the presence of IAA, FXIII was inhibited; therefore, only monomeric α2PI was observed, as no covalent cross-linking could occur. This non-covalently bound α2PI is presumably the NPB-α2PI form, as the PB-α2PI-specific antibody did not react with this band.

5.2.5 Clot lysis assay in artificial plasma samples

Our results indicated that plasma concentrations of PB-α2PI and NPB-α2PI forms correlate with clot lysis parameters, and that both forms are incorporated into fibrin clots, although in different ways. However, differences in α2PI N-terminal heterogeneity and other variables present in plasma samples greatly complicate the interpretation of effects derived specifically from C-terminal cleavage. To overcome this, we prepared plasma samples differing only in the amounts and ratios of α2PI C-terminal forms. α2PI-deficient plasma was supplemented with recombinant Met-PB- and/or Met-NPB-α2PI in varying ratios, and the clot lysis process from these samples was examined. Compared to α2PI-deficient plasma, the presence of both plasminogen-binding and non-binding α2PI forms prolonged lysis time. With 100% PB form (65 mg/L), CLT50 increased by 80% compared to α2PI-deficient plasma, while with 100% NPB-α2PI form (65 mg/L), lysis time increased by 30%. We also investigated the effect of increasing NPB-α2PI levels on lysis time while maintaining a constant PB-α2PI concentration. Increasing the proportion of NPB-α2PI led to a mild but statistically significant prolongation of lysis time. At the highest NPB-α2PI concentration, a 21% increase was observed compared to the 73:27% PB-α2PI:NPB-α2PI ratio.

5.2.6 Examination of fibrin network structure in artificial plasma samples

In the next step, α2PI-deficient plasma was supplemented with AF647-labeled fibrinogen, and various amounts of recombinant Met-PB- and/or Met-NPB-α2PI were added. After inducing clot formation, the clot's structure was analyzed using confocal laser scanning microscopy to examine the effects of different α2PI form ratios on the resulting fibrin clot architecture. For quantitative analysis, we determined the percentage of area coverage, pore size, and fibrin fiber thickness. Compared to fibrin clots formed without α2PI, the percentage of coverage significantly increased in the presence of PB and/or NPB forms, while pore size decreased, and thicker fibrin fibers were formed in clots supplemented with recombinant α2PI. The greatest structural changes relative to α2PI-deficient plasma were observed when both forms were present in proportions corresponding to those measured in normal plasma.

6. DISCUSSION

6.1 The effect of activated FXIII on smooth muscle cell functions

Vascular smooth muscle cells (VSMCs) are located in the medial layer of the vessel wall in a contractile phenotype. However, under certain physiological and/or pathological conditions and environmental stimuli, they could switch their phenotype. Injury, inflammation, or various growth factors can drive VSMCs to adopt phenotypes with distinct functions. The synthetic phenotype is most commonly activated during vascular injury or in atherosclerosis, playing an important role in tissue regeneration by promoting cell proliferation, migration, and collagen synthesis. In atherosclerosis and other inflammatory processes, VSMCs can also transform into an osteogenic phenotype. In the pathological, calcifying environment characteristic of atherosclerosis, VSMCs differentiate into osteoblast-like cells. Since cellular FXIII has been detected in osteoblasts, we first examined whether osteoblastic differentiation of VSMCs is associated with FXIII-A expression. However, osteoblastic transformation of VSMCs, confirmed by the expression of osteoblast-specific differentiation markers, was not accompanied by cellular FXIII expression. Therefore, VSMCs do not produce cFXIII; we next investigated whether externally added FXIII influences their functions. Extracellular FXIII in the vessel wall may be derived from plasma following vascular injury or rupture of an atherosclerotic plaque. It may also be released from activated platelets, macrophages accumulated in plaques, or from the cell surface itself. Thrombin generated within plaques can activate FXIII, which may in turn affect VSMC function. In the subsequent experiments, we studied the effects of FXIIIa on VSMCs, focusing on functions relevant to atherosclerosis and plaque development or maintenance. Specifically, we examined its impact on cell proliferation, *in vitro* wound closure, collagen secretion (a major component of the extracellular matrix), and TSP-1 expression. The proliferation assays showed that FXIIIa enhanced HAoSMC division even at concentrations below physiological plasma levels. These results were also supported by the *in vitro* wound closure assay, in which we demonstrated the combined effect of FXIIIa on cell proliferation and cell migration. Importantly, these cellular functions required the transglutaminase activity of FXIII, as non-activated FXIII did not influence VSMC migration or proliferation. Cell-specific effects of FXIII have previously been studied by Inbal and colleagues in other cell types. They reported that at higher concentrations (50 μg/mL), plasma FXIIIa enhanced endothelial cell migration and proliferation while reducing apoptosis. Similar effects

were observed in monocytes. The impact on fibroblasts was less consistent: FXIIIa significantly promoted migration of dermal fibroblasts but did not affect proliferation, while its effect on lung fibroblasts was only moderate compared to iodoacetamide-inhibited FXIIIa. FXIIIa can cross-link vitronectin receptors (αvβ3 integrins) and VEGFR-2 growth factor receptors on endothelial cells, leading to VEGFR-2 activation and initiation of angiogenesis-related signaling pathways (e.g., proliferation, migration). Since VSMCs also express vitronectin receptors, FXIIIa likely exerts similar effects on these cells. It should be noted that thrombin used for FXIII activation can itself influence VSMCs' functions. Therefore, in our experiments, thrombin activity was inhibited after the activation step, and results were compared with cells cultured in thrombin-inhibited medium. The effect of FXIIIa on collagen secretion has previously been studied in osteoblasts. Inhibition of FXIIIa (but not of transglutaminase 2) strongly inhibited osteoblast differentiation and mineralization, as well as fibronectin and type I collagen secretion and detachment from the cell surface. In our experiments, increased collagen production and incorporation into the extracellular matrix by HAoSMCs were observed when FXIIIa was added at concentrations above plasma levels. Lower FXIIIa concentrations were sufficient to enhance proliferation and migration. Thus, FXIIIa may contribute to phenotypic switching of VSMCs from a contractile, quiescent state to a synthetic phenotype, stabilizing plaques through increased collagen production and matrix incorporation. Several *in vitro* and *in vivo* studies have described the effects of FXIIIa on angiogenesis in relation to TSP-1 synthesis. In human endothelial cells treated with FXIIIa, TSP-1 mRNA expression was nearly abolished, and protein synthesis and secretion were reduced. *In vivo*, in the rabbit cornea, FXIIIa-induced angiogenesis was associated with TSP-1 deficiency. In another animal model, heterotopic heart transplantation in mice, FXIIIa treatment significantly reduced TSP-1 mRNA levels. FXIIIa thus influences key cellular components of atherosclerotic plaques, including endothelial cells, fibroblasts, and macrophages. We confirmed that FXIIIa also significantly affects VSMC functions, enhancing proliferation, migration, and collagen secretion. These properties play an important role in plaque stabilization and may even contribute to plaque growth. The effect of FXIIIa on TSP-1 expression in VSMCs appears more complex: TSP-1 levels in culture medium decreased markedly, potentially contributing to the pro-angiogenic effect of FXIIIa. However, this decrease was not associated with a reduction in synthesis, as seen in other cell types, but rather a portion of the secreted TSP-1 remained bound to the cells. Further studies are needed to clarify the role of cell-bound TSP-1.

6.2 The impact of α2-plasmin inhibitor heterogeneity on clot lysis and clot structure

α2-plasmin inhibitor (α2PI) undergoes proteolytic cleavage at both the N- and C-terminal ends in circulation, resulting in functional consequences. The N-terminal truncation is mediated by sFAP, resulting in an isoform that FXIIIa can crosslink to fibrin more rapidly. This mechanism has been studied by several groups, but less is known about the extent and impact of C-terminal cleavage. C-terminal modification can affect the efficiency of plasmin(ogen) inhibition, the extent and type of its incorporation into the fibrin clot, as well as the structure of the clot. Our study provides new insights by examining the plasma levels and relative ratios of intact and truncated C-terminal α2PI forms, and their incorporation into fibrin clots, as well as their effects on clot structure and lysis. Parallel measurement of α2PI activity and antigen concentration confirmed previous assumptions that activity strongly correlates only with PB-α2PI concentration. NPB levels had only a minor effect, and the relative ratio of the two forms in plasma did not influence measured α2PI activity. Previous reports on α2PI incorporation into fibrin clots have been highly dependent on the methods used. In one study using Laurell immunoelectrophoresis, total α2PI antigen levels in serum were reduced by 18 ± 9% (n = 12) compared to plasma, while immediate plasmin inhibition assays showed 35 ± 6% inhibition. In 65 blood donors, a 32.3% difference in α2PI activity was measured between plasma and serum. In clots dissolved in 6 M urea, only a small amounts of fibrin-bound α2PI were detected: 1.35 ± 0.18 mg/L out of 83.2 ± 15.4 mg/L total α2PI, measured by ELISA. Using a method developed by Uitte de Willige et al., the proportion of clot-incorporated α2PI was determined with fluorescently labeled α2PI-specific antibodies. In clots prepared from citrate-anticoagulated plasma of five healthy donors, 39 ± 4.9% bound α2PI was detected, of which ~90% was assumed to be cross-linked, since only 3.9 ± 0.5% was detected in the presence of FXIII inhibitor. These findings highlight the lack of a reliable method to distinguish between cross-linked and non-covalently bound α2PI in clots and to quantify their relative proportions.

In our study of 80 healthy volunteers, total, PB-, and NPB-α2PI antigen concentrations were measured in plasma and corresponding serum samples. Incorporation into clots was calculated as the difference between plasma and serum concentrations. The median (IQR) PB:NPB ratio in plasma was 2.1 (1.75–2.57), consistent with the ratio 2.2 (1.8–2.7) obtained by crossed immunoelectrophoresis using Lys-plasminogen in the first dimension gel. We found that 44.3 ± 6.3% of total α2PI remained in the clot after serum removal, higher than the commonly cited ~30%.

The PB:NPB ratio in clots was 1.37, indicating that NPB is incorporated into clots in significant amounts, even at higher relative proportions compared to its plasma concentration. Using Western blot to analyze intensively washed clots, we found that FXIIIa cross-links the PB form to the fibrin α-chains, after all was not detectable when bound to fibrin in a non-covalent manner, confirming earlier findings by Kluft et al. Polyclonal antibody labeling revealed non-cross-linked α2PI monomers even when FXIII was inhibited. This form is likely NPB, since PB-specific antibodies did not react with it. Consistent with this, plasma FXIII levels correlated significantly with PB, but not with NPB incorporation. Previous studies have demonstrated that FXIII-mediated cross-linking of PB-α2PI to fibrin is essential for preventing premature clot lysis. Surprisingly, however, neither FXIII plasma levels nor PB-α2PI concentrations correlated significantly with clot lysis time, though they did correlate with maximum absorbance. In contrast, NPB levels—both in plasma and incorporated into clots—showed significant associations with all three clot lysis parameters. To further investigate this effect, *in vitro* experiments were performed by supplementing α2PI-deficient plasma with recombinant full-length and/or C-terminally truncated α2PI. We examined the impact on clot structure and lysis time. Our results showed that NPB also prolonged clot lysis time, albeit to a much lesser extent than PB-α2PI. In the case when increasing amounts of NPB were added alongside a constant amount of PB form (equivalent to ~50% of normal plasma levels), a further elongation was observed in clot lysis time. Both α2PI forms influenced fibrin clot structure, increasing fibrin fiber thickness and reducing pore size. The greatest changes were observed when both forms were present in the amounts and proportions typical of normal plasma, which also supports the idea that the two forms bind to fibrin through different mechanisms, exert additive effects. Mechanisms that determine fibrin structure are not yet fully understood. However, numerous studies have reported alterations in fibrin structure associated with various thrombotic conditions. In several studies, reduced pore size, formation of thinner fibrin fibers, and reduced permeability have been linked to decreased fibrinolytic capacity and increased risk of thrombosis. Conversely, other studies report the formation of thicker fibrin fibers along with increased lysis time and reduced permeability. These latter findings support our results. However, in our case, the impact of clot structural changes on fibrinolysis caused by the binding of α2PI to fibrin cannot be separated from direct plasmin inhibition. It can be assumed that both mechanisms contribute to the reduction of the overall fibrinolytic capacity.

The quantity and ratio of C-terminal forms under pathological conditions have been examined in only two studies. Uitte de Willige et al. demonstrated an unchanged C-terminal cleavage ratio in the plasma of male survivors of myocardial infarction, despite reduced total α2PI levels. Barath B detected elevated total α2PI plasma levels following venous thromboembolism, which was due to an increase in the NPB form. Based on these results, it is also conceivable that C-terminal cleavage has different effects on the pathomechanisms of venous and arterial thrombosis. However, in the two studies mentioned, α2PI forms were determined only once after the thrombotic event, presumably not in the acute phase, which does not reflect the conditions corresponding to the acute event or the processes leading to it. An earlier study examined changes in PB and NPB -α2PI forms in plasma using a modified two-dimensional immunoelectrophoresis method and found that low-level plasminogen activation first reduced the amount of PB form in plasma, while higher-level plasminogen activation also reduced the amount of NPB form by 30%. This study did not examine the amount and effect of forms bound to the clot, but it draws attention to the fact that the effect of C-terminal forms is also influenced by the kinetics and extent of plasmin formation. This study did not examine the quantity and effect of forms bound to the precipitate, but it draws attention to the fact that the effect of C-terminal forms may also be influenced by the kinetics and extent of plasmin formation. Further studies, preferably prospective studies, are needed to clarify the pathological effect of C-terminal cleavage and, based on this knowledge, to develop possible therapeutic options. Based on our own results, we assume that C-terminal modification influences the effectiveness of plasmin inhibition, the type of incorporation into the fibrin clot, and the structure of the clot. There is a need to develop reliable methods for the direct determination of the forms incorporated into the clot.

This study should be interpreted in the context of its limitations. The study group is rather young, with a mean age of 33.2 ± 13.4 years, which could influence the generalizability of the results. The lack of reaction with the PB-α2PI-specific antibody is only indirect evidence that the PB variant is not present in the clot due to non-covalent binding to fibrin. It cannot be excluded that non-covalent binding to fibrin renders the epitope of the antibody used inaccessible. However, at present this is the only available antibody that recognizes the C-terminal end of α2PI and does not react with the non–plasminogen-binding form.

7. SUMMARY

Factor XIII exists in two forms: plasma (pFXIII) and cellular (cFXIII). The activated form (FXIIIa) ensures clot stability by cross-linking fibrin strands and binding α2-plasmin inhibitor (α2PI) to fibrin. It also plays a role in angiogenesis, wound healing, and maintenance of pregnancy. cFXIII can be detected in thrombocytes, monocytes/macrophages, and osteoblasts, among other cells. The direct effect of FXIII-A on endothelial cells and fibroblasts, which play a role in the formation of atherosclerotic plaques, has been demonstrated previously. Depending on environmental factors, vascular smooth muscle cells (VSMCs) can differentiate into osteoblast-like cells in plaques, so we investigated whether this differentiation is associated with FXIII-A expression and whether extracellular FXIII-A has an effect on the functions of VSMCs. Osteoblast transformation was not associated with cFXIII expression. Nonactivated FXIII-A did not affect the various functions of VSMCs. FXIIIa enhanced the proliferation of VSMCs even at concentrations lower than plasma concentrations. *In vitro* wound closure experiments confirmed the combined effect of FXIIIa on proliferation and migration. FXIIIa enhanced collagen synthesis and incorporation into the extracellular matrix. FXIIIa treatment did not alter the expression level of thrombospondin-1 (TSP-1), but the amount released into the medium decreased, with part of the TSP-1 formed remaining bound to the cells. These effects of FXIIIa may play a role in the pathogenesis of atherosclerotic plaques.

α2PI undergoes proteolytic cleavages in plasma, resulting in a heterogeneous structure with functional consequences. The form cleaved at the C-terminal end loses its plasminogen-binding site and is therefore much slower to inhibit plasmin (NPB-α2PI), while FXIIIa is primarily able to cross-link fibrin with the plasminogen-binding, uncleaved form (PB-α2PI). The effect of the NPB-α2PI form on fibrinolysis has been less studied. In our present work, we investigated the relationship between the amount of α2PI C-terminal isoforms and various plasma parameters, their incorporation into the fibrin clot, and their effect on the structure and lysis of the clot. The total α2PI incorporated into the clot was 44.3±6.3%, and the PB-α2PI:NPB-α2PI ratio was 1.37, indicating that a significant amount of NPB-α2PI also binds to the clot in a non-covalent manner. The plasma level of NPB-α2PI and the amount incorporated into the clot showed a significant correlation with clot lysis parameters (CLT50, MaxAbs, AUC). In *in vitro* experiments, the NPB form also prolonged clot lysis time, albeit to a lesser extent than PB-α2PI. Both C-terminal variants of α2PI affected the structure of fibrin clots, increasing the thickness of fibrin strands and reducing the pore size. According to our results, in addition to FXIIIa-crosslinked PB-α2PI, NPB-α2PI, which binds noncovalently to the clot, also affects the structure and dissolution of the clot; therefore, it would be worthwhile to further investigate the effect of heterogeneity in different pathological conditions.

8. NOVEL FINDINGS

1. The osteoblast transformation of human aortic smooth muscle cells (HAoSMCs) is not associated with FXIII-A expression, although FXIII-A is detectable in human osteoblast cells.
2. We have demonstrated that extracellular FXIII-A, following its activation, influences several functions of HAoSMCs in a concentration-dependent manner:
   - In cell proliferation assays, the activated recombinant FXIII-A (rFXIIIa) significantly enhanced proliferation even at a concentration below normal plasma levels.
   - *In vitro* wound closure assays have shown that rFXIIIa increased cell migration in a concentration-dependent manner.
   - rFXIIIa significantly increased collagen secretion by HAoSMCs.
   - Treatment with rFXIIIa did not increase TSP-1 gene expression in HAoSMCs, even at twice the plasma concentration. Nevertheless, we detected an increase in intracellular TSP-1 protein levels. Parallel to the increase in intracellular levels, TSP-1 decreased in the culture medium. These results suggest that rFXIIIa does not induce de novo synthesis of TSP-1 in HAoSMCs, but rather helps to retain it in the cytoplasm and is associated with the cell.
3. We examined the extent of incorporation of C-terminal α2PI forms (NPB-α2PI: non-plasminogen-binding, truncated form; PB-α2PI: plasminogen-binding, full-length form) into fibrin clots by analyzing clots prepared from normal human plasma. Contrary to previous assumptions, we found that NPB-α2PI also binds significantly to fibrin. Compared to their original plasma concentrations, NPB-α2PI is incorporated into the clot to a greater extent than PB-α2PI. The binding of NPB-α2PI to fibrin is a non-covalent interaction, in contrast to the covalent cross-linking of PB-α2PI mediated by FXIIIa. The binding of NPB-α2PI to fibrin occurs via non-covalent interactions, in contrast to PB-α2PI, which is covalently cross-linked to fibrin α-chains by FXIIIa.
4. In addition to the effect of cross-linked PB-α2PI on fibrin, the extent of NPB-α2PI incorporation also influences the plasmin-mediated clot dissolution. Both plasma levels and NPB-α2PI incorporated into the clot showed significant positive correlations with turbidimetric clot lysis parameters (CLT50, MaxAbs, AUC).

5. The impact of α2PI C-terminal variants on clot lysis was further confirmed using α2PI-deficient plasma supplemented with recombinant α2PI proteins.
6. Confocal microscopy analysis of fibrin network structure revealed that binding of PB and/or NPB-α2PI to the clots results in the formation of thicker fibrin fibers and reduced pore size of the fibrin network.

9. ACKNOWLEDGEMENT

First and foremost, I would like to express my gratitude to my supervisor, **Dr. Éva Katona**, who supported me throughout this long journey with her valuable advice and professional guidance. Her experience and commitment to excellence have enriched my approach to research. I greatly appreciate her encouragement, patience, and, last but not least, her help in preparing my dissertation.

I am grateful to **Professor László Muszbek** for giving me the opportunity to participate in his research project, the results of which I was able to present at numerous conferences both in Hungary and abroad. Without his support, the paper on the effects of FXIII, which forms the basis of my dissertation, would not have been possible.

I would like to thank **Dr. Zsuzsanna Bereczky**, head of the Division of Clinical Laboratory Science, who stood by me throughout, enabling me to complete my PhD work.

I would like to thank **Prof. Dr. László Góth** and **Dr. Teréz Nyesténé Nagy**, the mentors of my first scientific work, who launched my research career and have accompanied my work ever since.

I would also like to thank all my co-authors and colleagues for their valuable and dedicated work in contributing to the preparation of these publications. I am especially grateful to **Dr. Barbara Baráth** for our successful collaboration.

I would like to thank **my colleagues**, whom I consider my friends. I am grateful to be part of such an inspiring, supportive, and cheerful work community.

Finally, I am grateful to **my friends and family**, whose encouragement gave me strength during this period. To **my husband** and **my two mischievous children**, who believed in my goal. However, my greatest supporters in life are **my parents**, who always stand by me with their endless patience and devoted love. I hope they are proud of me now, too!

Applications supporting research: NKFIH (K129287, K120633, K139293); GINOP 2.3.2-15-2016-00050, a project co-financed by the European Union, the European Regional Development Fund, and the Hungarian Academy of Sciences (11014); DE Scientific Research Fund (DETKA), MTA-DE Momentum (LP2024-1/2024).

10. LIST OF PUBLICATIONS

UNIVERSITY of DEBRECEN

UNIVERSITY AND NATIONAL LIBRARY
UNIVERSITY OF DEBRECEN
H-4002 Egyetem tér 1, Debrecen
Phone: +3652/410-443, email: publikaciok@lib.unideb.hu

Registry number: DEENK/530/2025.PL
Subject: PhD Publication List

Candidate: Réka Kissné Bogáti
Doctoral School: Kálmán Laki Doctoral School

List of publications related to the dissertation

1. **Kissné Bogáti, R.**, Baráth, B., Pituk, D., Orbán-Kálmándi, R. A., Szűcs, P., Hegyi, Z., Bereczky, Z., Bagoly, Z., Katona, É.: Effect of Alpha2-Plasmin Inhibitor C-Terminal Heterogeneity on Clot Lysis and Clot Structure.
   Biomolecules. 15 (8), 1-16, 2025.
   DOI: http://dx.doi.org/10.3390/biom15081127
   IF: 4.8 (2024)
2. **Kissné Bogáti, R.**, Katona, É., Shemirani, A. H., Balogh, E., Bárdos, H., Jeney, V., Muszbek, L.: The Effect of Activated FXIII, a Transglutaminase, on Vascular Smooth Muscle Cells.
   Int. J. Mol. Sci. 23 (10), 1-15, 2022.
   DOI: http://dx.doi.org/10.3390/ijms23105845
   IF: 5.6

List of other publications

3. Kállai, J., Gindele, R., Pénzes-Daku, K., Balogh, G., **Kissné Bogáti, R.**, Bécsi, B., Katona, É., Oláh, Z., Ilonczai, P., Boda, Z., Róna-Tas, Á., Nemes, L., Marton, I., Bereczky, Z.: Clinical and Molecular Characterization of Nine Novel Antithrombin Mutations.
   Int. J. Mol. Sci. 25 (5), 1-19, 2024.
   DOI: http://dx.doi.org/10.3390/ijms25052893
   IF: 4.9
4. Pituk, D., Balogh, L., Horváth, E., Hegyi, Z., Baráth, B., **Kissné Bogáti, R.**, Szűcs, P., Papp, Z., Katona, É., Bereczky, Z.: Localization of Hemostasis Elements in Aspirated Coronary Thrombi at Different Stages of Evolution.
   Int. J. Mol. Sci. 25 (21), 1-19, 2024.
   DOI: http://dx.doi.org/10.3390/ijms252111746
   IF: 4.9

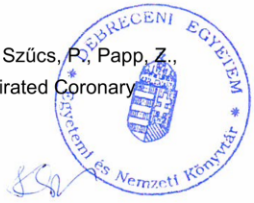

UNIVERSITY of DEBRECEN

UNIVERSITY AND NATIONAL LIBRARY
UNIVERSITY OF DEBRECEN
H-4002 Egyetem tér 1, Debrecen
Phone: +3652/410-443, email: publikaciok@lib.unideb.hu

5. Baráth, B., **Kissné Bogáti, R.**, Miklós, T., Kállai, J., Mezei, Z. A., Bereczky, Z., Muszbek, L., Katona, É.: Effect of [alfa]2-plasmin inhibitor heterogeneity on the risk of venous thromboembolism.
   Thromb. Res. 203, 110-116, 2021.
   DOI: http://dx.doi.org/10.1016/j.thromres.2021.05.003
   IF: 10.407

6. Bagoly, Z., Baráth, B., Orbán-Kálmándi, R. A., Szegedi, I., **Kissné Bogáti, R.**, Sarkady, F., Csiba, L., Katona, É.: Incorporation of [alfa]2-Plasmin Inhibitor into Fibrin Clots and Its Association with the Clinical Outcome of Acute Ischemic Stroke Patients.
   Biomolecules. 11 (3), 1-13, 2021.
   DOI: http://dx.doi.org/10.3390/biom11030347
   IF: 6.064

7. Gindele, R., Pénzes-Daku, K., Balogh, G., Kállai, J., **Kissné Bogáti, R.**, Bécsi, B., Erdődi, F., Katona, É., Bereczky, Z.: Investigation of the Differences in Antithrombin to Heparin Binding among Antithrombin Budapest 3, Basel, and Padua Mutations by Biochemical and In Silico Methods.
   Biomolecules. 11 (4), 1-18, 2021.
   DOI: http://dx.doi.org/10.3390/biom11040544
   IF: 6.064

Total IF of journals (all publications): 42,735
Total IF of journals (publications related to the dissertation): 10,4

The Candidate's publication data submitted to the Tudóstér have been validated by DEENK on the basis of the Journal Citation Report (Impact Factor) database.

19 September, 2025

DEBRECENI EGYETEM * Egyetemi és Nemzeti Könyvtár *